2011 International Conference on Telecommunication Technology and Applications
Proc .of CSIT vol.5 (2011) © (2011) IACSIT Press, Singapore

A Recognition System for 3D Embossed Digits on Non-Smooth Metallic Surface

Taweepol Suesut , Suphan Gulpanich and Kitti Tirasesth

Department of Instrumentation and Control Engineering,
Faculty of Engineering, King Mongkut's Institute of Technology Ladkrabang,
Bangkok 10520 THAILAND

Abstract. This paper presents a new solution to the automatic localization and recognition of natural digits embossed on structured and rough surfaces. A new concept of combining periodic (e.g. FFT, DCT) with polynomial moments (e.g. Tchebichef moments) is shown that the new method can eliminate some of the problems associated with the Gibbs phenomena. QR decomposition is used to obtain a unitary basis, minimizing the numerical effort when modeling surfaces. The combined moment method is used to generate a smoothed global model of the surface structure. Following segmentation of the individual digits, pattern recognition based on moment function such as Hu's moment invariants, Zernike moments, and Orthogonal Fourier Mellin Moments was used to recognize the stamped number after analyzing 3D surface data of the steel block. A prototype system of the laser-scanning instrument was implemented and test measurements were performed in a production line. The results showed the correct functionality of the method.

Keywords: Polynomial moments, 3D surface modeling, OCR, machine vision, Gibbs error

1. Introduction

Most steel production plants produce steels of different qualities containing various alloys. Consequently, for critical products, such as oil drilling rods, it is essential to track the steel from the continuous caster to its use in an individual product. Only in this manner can the quality of the material be ensured. The difficulties associated with material tracking in steel production are: the material needs to be marked at temperatures of up to 1100±C, which precludes the use of classical labels; there is significant growth of scale, particularly for high carbon steels. As a result the marking must be robust enough to withstand later rescaling - commonly performed with water jets at 2000 Bar; thermal stress during cooling may lead to significant deformation of the product; the ends of the bars are cut using autogenic-burners, which leaves a characteristic rough surface (see Figure 1a). Presently the solution to these problems is to emboss a code as a 3D structure into the surface of the material.

There has also been a migration of the types of embossed codes used: originally, embossed dot or bar codes were used. These codes are not human-readable which proved to be a major disadvantage. It is very difficult to maintain tracking of steel bars which are removed from the plant during unplanned disruption of the production. Later the bars were embossed with both human-readable and machine readable codes; see Figure 1a for an example. The reason for stamping both codes was that there were no reliable methods to locate and identify the natural digits on such rough surfaces.

In general, character recognition or optical character recognition (OCR), sub-field of pattern recognition, is applied with a binary image acquired by scanner or digital camera. Using a camera to directly capture images from metallic surface is very difficult to perform image segmentation and classification. Because of the image of metallic surface in this work is dark and contains a periodic texture, global deformations, and local anomalies - characteristics. It is not easy to classify the number stamped on the metallic surface by a simple technique.

Typically, a character recognition system comprises three main steps: pre-processing, feature extraction, and classification. After performing the surface relief, the image of surface is manipulated by a variety of

methods that perform operations such as filter for noise removal, image enhancement and segmentation. This stage ensures that the resultant image is made suitable for further processing.

(a)

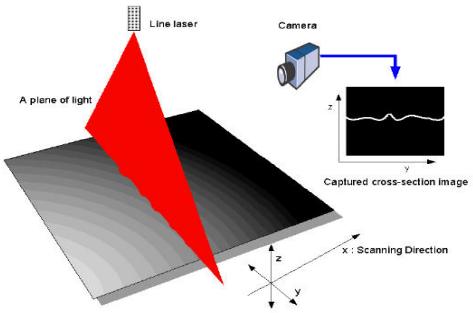

(b)

Fig.1 a) Examples of an embossed bar code combined with embossed natural digits. b) 3D surface data acquisition using laser light sectioning.

2. Moments for surface modeling

As the steel bar enters the production line it is stopped briefly, and the geometry of the end of the bar is measured by a 3D scanner. The scanner (see Figure 1b) consists of a linear drive which moves a laser plane-of-light measurement unit past the surface. A complete 3D geometry of the surface containing the embossed code is acquired (see Figure 1a). The reconstruction of the 2D cross sections from the images can be constructed of a 3D surface from the individual cross sections.

This paper presents a solution to the automatic localization and recognition of natural digits which are stamped as 3D structures on rough surfaces. Recently, discrete polynomial moments were applied to real-time geometric surface inspection [1][2][3]. This paper builds upon that recent work extending the technique to combine discrete polynomial and periodic bases in a single new unitary basis; efficiently dealing with surfaces having a combination of periodic texture, global deformations and local anomalies – characteristics are typical of parts produced by mechanical machining. Since the combined moment method has been applied to enhance the surface information, images of stamped number are able to perform pattern recognition algorithms.

2.1 Polynomial moments

It has been proved that there is one and only one discrete unitary polynomial basis [4]. The unique unitary polynomial basis P, a sum of monomials, can be synthesized in the range [-1, 1] directly from the recurrence relationship,

$$P_n = \alpha p_1 \circ p_{n-1} + \beta p_{n-2} \tag{1}$$

whereby,

$$\alpha = \frac{1}{\sqrt{p_t^T p_t - (p_t^T p_{n-2})^2}} \tag{2}$$

and

$$\beta = \alpha p_t^T p_{n-2}, \tag{3}$$

given

$$p_0 = \frac{1}{\sqrt{N}}, \text{ and } p_1 = \sqrt{\frac{3(N-1)}{N(N+1)}}x. \tag{4}$$

The individual column vectors p_i are concatenated to form the complete polynomial basis of degree n, i.e P = [p_0 .... p_n]. This polynomial basis forms a Tchebychev system, the basis is unitary $P^T P = I$ Low degree polynomial moments can model the gradients and sub-harmonic components of data well.

2.2 Combined moments

The new concept is to combine a polynomial and a periodic basis to form a new basis, which is better suited for modeling data with a combination of periodic and non periodic components. Consider, the concatenation of a polynomial and cosine bases to form a new basis set,

$$B = [P, C]. \tag{5}$$

The bases P and C are both unitary; however, they are not orthogonal to each other $P^T C \neq 0$ In this case perfect reconstruction requires the computation of the pseudo inverse of B,

$$\hat{y} = BB^+ y. \tag{6}$$

It can be proved [6] that a QR decomposition exists for any real matrix, such that,

$$B = QR, \tag{7}$$

where Q is a unitary matrix and R is an upper triangular matrix. Note: for an appropriate QR algorithm $Q^T Q = I + E,$ with $\|E\|_2 \approx u$ the numerical resolution of the computer.

Furthermore,

$$BB^+ = QQ^T \tag{8}$$

In further computations Q is used as the orthogonal basis.

2.3 Extension to 3D data

Separable orthogonal bases are used to model 3D surfaces. Eden et al. 1986 [5]showed that the computation

$$\hat{Z} = YMX^T, \tag{9}$$

performs a least square approximation $\hat{Z}$ of Z, whereby X and Y are the bases used in the x and y directions respectively. The bases in x and y may and commonly are different. In the case of a unitary polynomial basis $P^+ = P^T$ the reconstruction process becomes,

$$\hat{Z} = YY^T Z(XX^T)^T. \tag{10}$$

In the application tested here the residual surface is computed as,

$$R = Z - YY^T Z(XX^T)^T. \tag{11}$$

The aim is to separate the low degree geometric deformation of the surface and the periodic portion of the surface from the remaining data. This enables the detection of local anomalies. The data set consists of 611 by 591 points. Figure.2a shows the original data from the 3D scanning instrument. The residual after removal of the surface model associated with the combined moments, (polynomial components dx = 5, dy = 5 and cosine components cx = 6…36, cy = 5…10) has been illustrated in figure 2b.

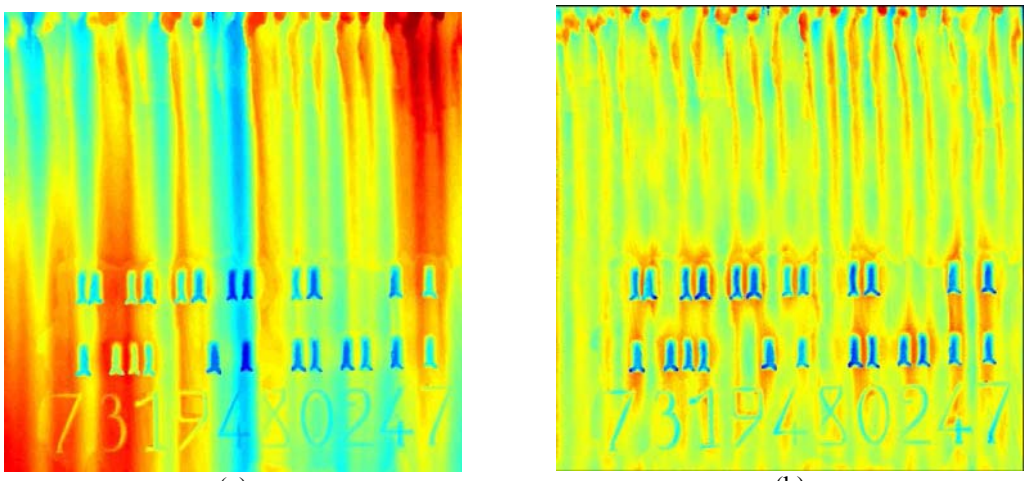

(a) (b)

Fig.2. a) Original data b) Residual after removal of the surface model associated with the combined moments

3. Pattern recognition based on moment invariants

In this work, images of number are computed to the moments feature vectors; there are three types of moment are adopted, i.e. Hu's moment invariants, Zernike moments, and Orthogonal Fourier Mellin Moments. These feature vectors of the image of the number are constituted by invariant functions of moments of different orders, so that the global shape characteristics of the image are invariant with translation, rotation and scale.

Moments of different orders usually exhibit large dynamic range variations. This leads to the domination of a subgroup of features among a set of moments. Therefore, the moments in a feature vector have to be appropriately weighted to get balanced representation of different components of the image shape. Higher order moments are more sensitive to image noise and quantization effects, and can lead to mismatch in pattern recognition algorithms. Moment of orders higher than four is not commonly used in feature vector construction.[7]

An appropriate feature vector for the pattern matching of the number is selected according to the following cases. In case of Hu moments, the feature vector Z was formed from all seven Hu's moments [8] as defined by equation (12)

$$z = \{H_i, i = 1,...,7\}. \tag{12}$$

In case of Zernike moments [10] (A. Khotanzad et al. 1990), the feature vector of absolute Zernike moment values was constructed as defined by equation (13)

$$z = \{Z_{ij}, i = 0,...,4 \wedge (i-j) = 2^k, k \in N\}. \tag{13}$$

In case of Orthogonal Fourier-Mellin moments,[9] the feature vector values were defined by equation (14). The circular Fourier or radial Mellin moments (FMMs) of an image function $f(r,\theta)$ was defined in the polar coordinate system (r,θ) as

$$F_{p,q} = \int_0^{2\pi}\int_0^{\infty} r^p f(r,\theta) e^{(-jq\theta)} r dr d\theta. \tag{14}$$

Where $q = 0, \pm 1, \pm 2$ is the circular harmonic order and the order of the Mellin radial transform is an integer p with $p \geq 0$.

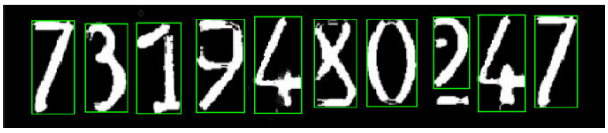

Fig.3 Images of number after enhancing.

4. Experimental results

The experiment performs according to the 3D surface recognition procedure. After surfaces of the steel block were acquired by the light sectioning instrument, surface approximation to surface relief by combined moments was done. Subsequently, images of surface were performed image pre-processing (i.e. noise removal, segmentation) to finally located the numbers on the images using labeling algorithm by 8-pixels-neighbors as shown in figure 3. The recognition of the number could be well done except the number with some missing part. To illustrate the performance of the classification and recognition, the artificial samples of image were made for various forms (e.g. rotation, missing part). There are three kinds of moment invariants i.e. Hu moment (HMI), Zernike moment (ZMI) and Orthogonal Fourier-Mellin moment (OFMMI) in this experiment. In order to test the recognition accuracy, two experiments were done to compare the performance of selected moment invariants. Firstly, testing recognition rate was performed with adding "salt and pepper" noise at different levels of noise (i.e. 1%, 2%, 3%, 4%) to the samples. Secondly, the sample images were rotated with every 10 degree of rotation. The results are shown in Table 1 and Table 2.

Table 1 Comparison of recognition rate of HMI, ZMI AND OFMMI with noise adding into image

Moments	*0% of Noise*	*1% of Noise*	*2% of Noise*	*3% of Noise*	*4% of Noise*
HMI	98	78	41	29	16
ZMI	98	98	98	98	91
OFMMI	98	81	66	59	55

Table 2 Recognition results of moments with rotated images

Moments	*Recognition rate (%)*
HMI	71
ZMI	79
OFMMI	42

5. Conclusion

The work presented in this paper has focused on the geometric modeling to enable a robust extraction of the digits from the structured and rough surface. It has been shown that combining polynomial and periodic moments leads to more efficient modeling of real machined surfaces. The Gibbs energy associated with simple gradients in the signal or sub-harmonic components can be eliminated (Paul O'Leary et al. 2008). The new basis is unitary which ensures the best numerical performance, while minimizing the propagation of errors associated with doing operations on poorly conditioned matrices. The new method enables the separation of global geometric form from periodic undulations and local anomalies.

A recognition system of stamped number on metallic surface using moment invariants has been implemented. The classifiers were implemented using Euclidean distance measure. Moments can be applied well not only in the smooth surface approximation for geometric surface inspection but also in the pattern recognition. The results presented here indicate that three types of moment invariants i.e. Hu moments, Zernike moments, and Orthogonal Fourier-Mellin moments are useful for recognizing of the number. In case

of the samples without some missing part, the recognition by adding noise "salt and pepper" could be well done for the Zernike moments. Hu's moment invariants were low performance when applied with noisy image. When the samples with some missing part were applied, OFMM invariants were low recognition rate. However, these moments are suitable for a small size image (Y.Sheng et al. 1994). The Zernike moments were still the best performance.

6. References

[1] Taweepol Suesut, Peter Schalk, Paul O'Leary, Ewald Fauster, Matthew Harker (2007) Real-time Geometric surface Inspection. International Conference on Engineering, Applied Science and Technology, Thailand

[2] F. Pernkopf and P. O'Leary (2003) Image acquisition techniques for automatic visual inspection of metallic surfaces. NDTE International, vol. 236, pp.609–617.

[3] Paul O'Leary, Matthew Harker, Taweepol Suesut (2008) Combined Polynomial and Periodic Moments for the Analysis of Measured 3D surfaces.I2MTC 2008 International Instrumentation and Measurement Technology Conference,Victoria,Canada

[4] Paul O'Leary and M. Harker(2009) Discrete polynomial moments for real-time geometric surface inspection. Journal of Electronic Imaging, vol.18, pp. 1–38.

[5] M. Eden, M. Unser, and R. Leonardi (1986) Polynomial representation of pictures. Signal Processing vol. 10, pp. 385–393

[6] G. Golub and C. Van Loan (1996) Matrix Computations, 3rd ed. Baltimore: John Hopkins University.

[7] R. Mukundan and K. R. Ramakrishnan (1998) Moment functions in image analysis,Theory and Applications. Singapore: World Scientific.

[8] M.-K. Hu (1962) Visual pattern recognition by moment invariants. IRE Transactions on Information Theory, pp. 179–187.

[9] Y. Sheng and L. Shen (1994) Orthogonal fourier-mellin moments for invariant patter recognition. Journal of Optical Society of America, vol. 11, pp. 1748–1757.

[10]A. Khotanzad and Y. Hong (1990) Invariant image recognition by zernike moments. IEEE Transaction on Pattern Analysis and Machine Intelligence, vol. 12, pp. 489–498, 1990.